Modeling of Binding Modes and Inhibition Mechanism of Some Natural Ligands of Farnesyl Transferase Using Molecular Docking

Alessandro Pedretti, Luigi Villa, and Giulio Vistoli*

Istituto di Chimica Farmaceutica e Tossicologica, University of Milan, Viale Abruzzi 42, I-20131 Milan, Italy

Received October 26, 2001

Several natural inhibitors of farnesyl transferase have been reported in the literature: some compounds are competitive with farnesyl pyrophosphate (FPP), whereas other ones are competitive with Ras proteins, even though it is usually hard to highlight their inhibition mechanism, which is still unknown for several natural compounds. The aim of this work is to show that the molecular docking analysis can be successfully used to underline the inhibition mechanism of these natural compounds. First, the selected compounds were subjected to a detailed docking analysis, by means of BioDock, a program able to reveal the most likely binding mode for each ligand. By comparing these results with the binding sites for the natural substrates, earlier determined, it was possible to highlight the site specificity and the inhibition mechanism of the selected compounds. In addition, it is possible to relate the binding mode of these molecules with their lipole values, which is appreciably less for peptidomimetics than for FPP mimetic and reveals a straightforward method to predict and to understand the inhibition mechanism of these natural derivatives.

Introduction

Ras proteins are guanine nucleotide (GTP) binding proteins that play a pivotal role in mitotic signal transduction. In normal cells, the GTPase subunit, included in the Ras structure, controls Ras activity, promoting the formation of the inactive Ras-GDP complex.[1]

Mutated forms of Ras protein are found in approximately 30% of all human cancers.[2] These oncogenic proteins, which are lacking in GTPase activity, are irreversibly complexed with GTP.[3] This discovery has induced many laboratories to explore the role of Ras-induced cellular transformations in order to find novel anticancer therapeutics. In this regard, the posttranslational modifications have attracted great attention, being required for appropriate subcellular localization of Ras proteins in the plasma membrane.[4]

The first and mandatory step in the posttranslational modifications is the farnesylation on the thiol group of a cysteine located at the Ras C-terminus through a thioether bond. This residue is a part of the recognition sequence Ca_1a_2X found in many mammalian proteins.[5]

The transfer of the farnesyl moiety from farnesyl pyrophosphate (FPP) to the Ras protein is catalyzed by farnesyl protein transferase (FTase), which, like geranylgeranyl transferase I (GGTase I), recognizes the appropriate Ca_1a_2X consensus motif, where a_1 and a_2 are aliphatic amino acids and X sets out the specificity for the two prenyltransferases.[6]

Several studies showed that the FTase inhibition blocks Ras-induced biological transformations,[7] whereas the following posttranslational modifications, including removal of a_1a_2X tripeptide by proteolytic cleavage, methyl esterification of the new C-terminus,[8] and palmitoylation,[9] are not essential for the Ras proteins activity.

The crystal structure of FTase was recently published at 2.25 Å resolution.[10] FTase is a zinc heterodimeric metalloenzyme consisting of two subunits: the first weights 48 kD (α)[11] and the later 46 kD (*β*).[12] The zinc ion is placed at a junction between a hydrophilic surface of the α subunit and a deep cleft in the *β* subunit lined by aromatic residues. The zinc is coordinated by Asp297*β*, Cys299*β*, His362*β*, and a water molecule.

The FTase substrates can be investigated as models for designing selective FTase inhibitors,[13] and thus all novel inhibitors can be classified as (1) molecules designed on the Ca_1a_2X motif (peptidomimetics), which interact with the same FTase residues involved in Ras protein binding,[14] (2) molecules designed on the Farnesyl moiety (FPP mimetics), which interact with the FPP binding site,[15] and (3) bisubstrate inhibitors, which incorporate structural motifs of both FPP and Ca_1a_2X tetrapeptide.[16−19]

Several natural inhibitors of FTase have been reported. Some are competitive with FPP, while others are competitive with Ras proteins, but usually it is harder to highlight their inhibition mechanism, which is still unknown for several natural compounds.

Aim of this work is to show that the molecular docking analysis can be successfully used to underline the inhibition mechanism of several natural compounds.

In this research, we have analyzed molecules that are clearly FPP mimetics, like schizostatins, molecules that are competitive with Ras protein binding site, like artemidolide, and other compounds, whose mechanism is not yet clear or unidentified, like steroidal analogues.

The selected compounds were subjected to a detailed docking analysis using BioDock[20]—an automatic stochastic docking program—in order to bring to light the most likely binding modes for each ligand. By comparing

* Correspondence should be addressed to Giulio Vistoli, tel +39-02-50317522; fax +39-02-50317565; e-mail giulio.vistoli@unimi.it.

10.1021/jm011075w CCC: $22.00
Published on Web 02/21/2002

these results with the binding sites for the natural substrates, earlier determined,[33] it was possible to reveal the inhibition mechanism for the examined derivatives.

Computational Details

FTase Crystal Structure Refinement. The crystal structure of rat FTase, resolved by Park et al.,[10] is available in the Protein Data Bank (entry code 1FT1). The structure file contains the coordinates of protein heavy atoms (except for the first 55 residues of α subunit) and 401 water molecules that were preserved during all simulations performed in this study to shield the polar residue on protein surface and to smooth the polar interactions. The charge of Zn^{2+} is set to +2, and we use for it the CHARMm parameters determined by Fantucci et al.[21] In all simulations, the Zn^{2+} is coordinated with Cys353*β*, Asp57*β*, and His68*β*, while the water molecule was deleted to allow the interaction with ligands.

The force field CHARMm[22] v22 was used to assign partial charges to the protein and, after adding all hydrogen atoms (residues Arg, Lys, Glu, and Asp were considered ionized, while all His were considered neutral by default), the protein structure was minimized using both steepest descent algorithm until RMS = 0.5 and conjugated gradients until RMS = 0.01, keeping the backbone constrained to preserve the experimental structure.

We use in all calculations the apo enzyme form (and not the FTase-FPP complex) even if it is well-known that the FPP interaction alters the topology of the peptide binding site, because we must have both binding sites free and able to interact with the ligand in order to elucidate its inhibition mechanism.

Natural Compounds Construction. The conformational analysis of all natural ligands was performed using high temperature (2000 K) molecular dynamics (500 ps), which is able to span the conformational space of flexible molecules. The best structure obtained in this way was finally optimized by MOPAC 6.0[23] (keywords = AM1, PRECISE, GEO-OK).

Docking Analysis. All docking searches were performed using BioDock, a self-made tool, previously tested in several docking studies. This software performs automated docking of ligands to biomacromolecules, using a stochastic approach and keeping rigid both the interaction partners during the calculations. BioDock randomly rototranslates the ligand position into user-defined ranges. After discarding bumping positions, the obtained orientations are ranked using the nonbond intermolecular CVFF energy, like score function, and the analogous positions are clustered in a few noteworthy solutions saved in an output trajectory file. The main logical components are depicted in Chart 1. The ranges used to dock the substrates into the FTase structure were equal to 360° for the rotations and to 30 Å for the translations. The dielectric constant was set to 30 to take off the low polarity of the enzyme cavity and to reduce the polar interactions. All docking calculations obtained approximately 10 000 000 random orientations clustered in about 50 interesting groups. In the clustering analysis the ligand is reduced to a spheroid, defined by a set of pseudo-coordinates, to reduce the computational time. The clustering algorithm calculates the distance between pairs of spheroid of each orientations, and if this measure is less than a user-defined cutoff the last result is discarded. The five best solutions are optimized with BioDock, using a local search algorithm, which uses closer rototraslational ranges (30° and 5.0 Å) and reduces them until the energy converges.

The best solution obtained was minimized, using a computational procedure made up of two minimization processes. The first minimization was performed using steepest descent algorithm with backbone constrained until RMS = 0.5; the second uses the conjugated gradient until RMS = 0.01, keeping all atoms fixed outside a 15 Å radius sphere around the ligand.

Except for the calculations performed using BioDock or MOPAC 6.0, all of them were performed using Quanta/CHAMm.[24] All the software was implemented on SGI R4400 Indigo^2 workstation. BioDock[25] is a C written software developed using the Software Development Kit (SDK) of Irix6.2.

Chart 1. Main Logical Components of the BioDock Program

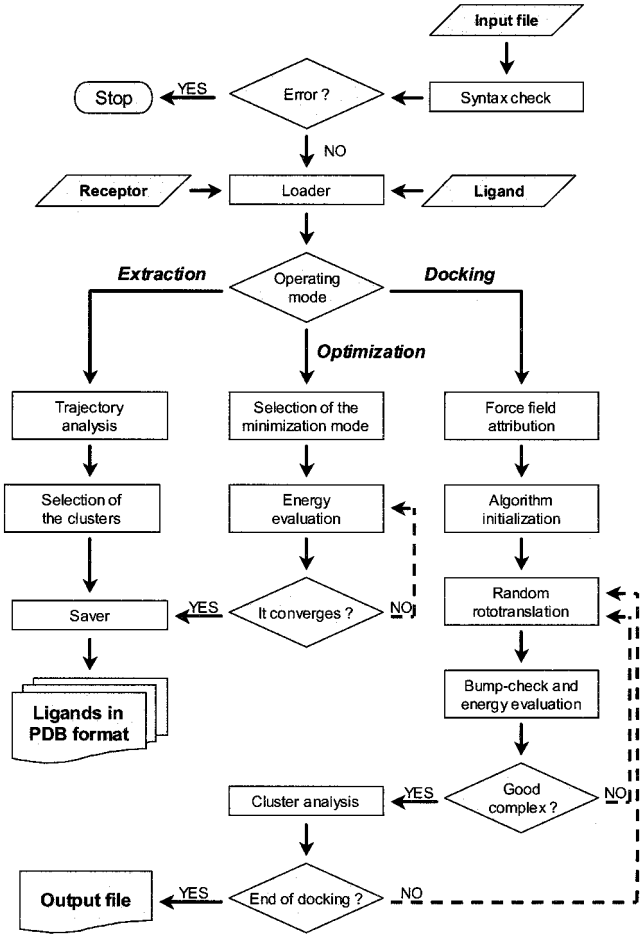

Docking Results

In Chart 2 are reported the natural compounds that were analyzed in this study with their inhibition activities (IC_{50} values). All compounds were considered preserving the complete configuration reported in the literature. In particular, when the configuration of all stereocenters is not reported, as in the case of clavaric acid derivatives, all possible stereoisomers were analyzed.

Zaragozic Acid.[26] The remarkable size of this statin, produced by a species of *Phoma*, justifies his poor site specificity. Indeed it interacts with residues of both FPP binding sites, as the interactions between carboxyl groups and Zn^{2+} ion or Lys-164α, and the Ras protein binding site, as the H-bonds between oxygenated functions and Tyr-361*β*, His-362*β*, and Ser-357*β* (Figure 1). The capability of interacting with several residues of both binding sites can explain the good inhibition activity of this compound.

Fusidienol.[27] Despite its smaller size, this molecule, isolated from *Fusidium coccineum*, is able to occupy both binding sites. It interacts with Zn^{2+} ion, and it forms H-bonds with Tyr-300*β* and His-248*β*. Importantly, the oxygen atoms, which interact with Zn^{2+} ion, are intranular, while the carbonyl groups, more electronegative, interact with cationic residue (Arg-291*β*). These interactions dock the fusidienol in a particular position that shields the Zn^{2+} ion to the natural substrates (Figure 2).

Chart 2. Molecular Structure of the Natural Compounds Considered with Their Inhibition Activities

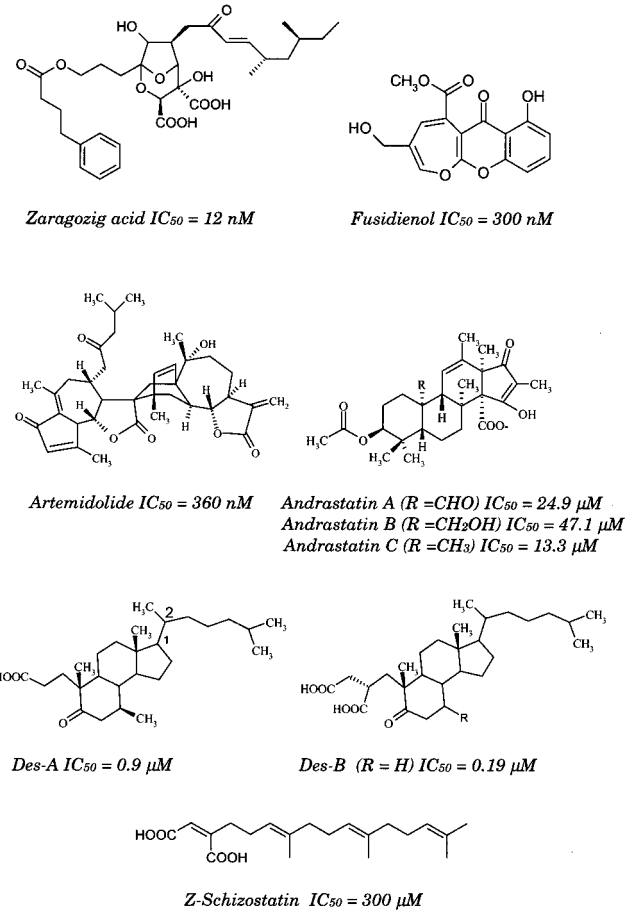

Artemidolide.[28] This compound, extracted from *Artemisia sylvatica*, shows an interesting activity and selectivity versus FTase. The obtained complex is stabilized by a lot of H-bonds, which involve the oxygenated functions of artemidolide and the residues Tyr-361β, Tyr-300β, His-362β, and Ser-357β. In this complex, the inhibitor does not interact directly with Zn^{2+} ion.

Schizostatin.[29] The two geometric isomers of this compound isolated from *Schizophyllum commune* are good inhibitors of squalene synthase and weak FTase inhibitors. These molecules show a particular stereoselectivity, being the only *Z*-isomer active versus FTase, while the other isomer is totally inactive. This selectivity is justified by docking results: in the *Z*-isomer complex, only the two carboxyl groups interact directly with the Zn^{2+} ion, while the *E*-isomer does not interact with Zn^{2+} ion.

Andrastatins.[30] The three molecules, isolated from a species of *Penicillum*, have a gonanic backbone and show poor FTase inhibition activities. Docking analysis shows different interaction patterns between the three compounds and the enzyme, and these divergences can justify their different activities. Indeed, the two most active compounds (Andrastatin A and Andrastatin C) form an ion pair between carboxyl group and Zn^{2+} ion, while the Andrastin B does not realize it. These results underline the relevance of this electrostatic interaction. The H-bonds concur to stabilize the FTase-andrastatin complexes. In particular, Andrastatin A and C realize

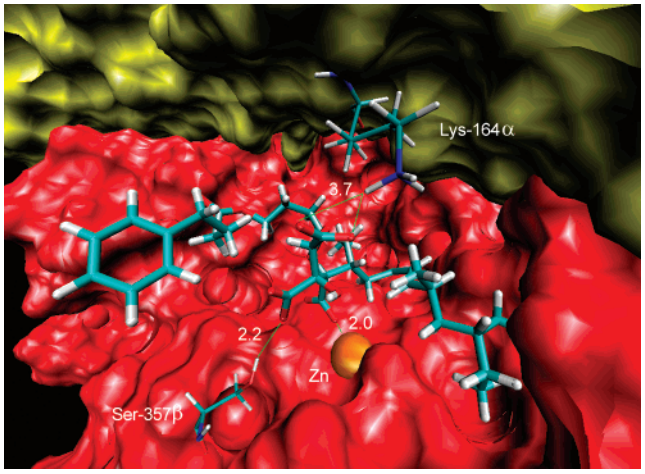

Figure 1. Main interactions between zaragozic acid and FTase. The electrostatic interaction between the carboxylic function of the ligand and the Zn^{2+} ion or Lys-164α is remarkable. The α subunit is shown in yellow and the β subunit in red.

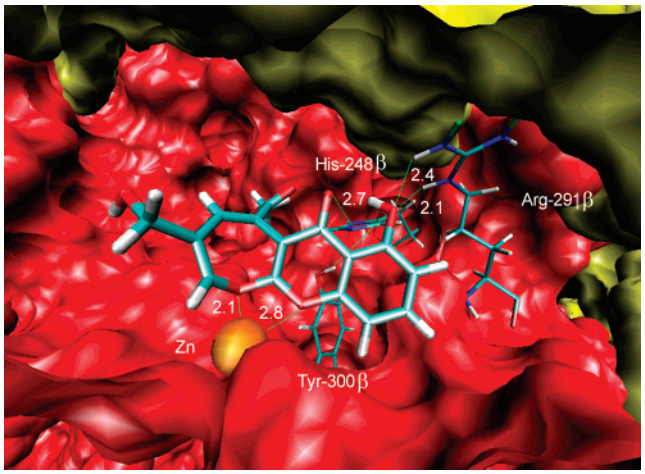

Figure 2. Main interactions between fusidienol and FTase. Note the electrostatic interactions between the carbonyl groups of ligand and Arg-291β, while the Zn^{2+} interacts with the intraanular oxygen atoms. The α subunit is shown in yellow and the β-subunit in red.

three H-bonds that involve the acetoxyl group, the carboxyl moiety, and the hydroxyl with, respectively, Cys-95β, Tyr-300β, and Ser-357β (Figure 3), while the complex between Andrastatin B and FTase becomes stable for a Coulombic interaction between the carboxyl moiety and Lys-164α, reinforced by three H-bonds between (1) the carbonyl group and His-362β, (2) the hydroxymethyl group and Ser-357β, and (3) the hydroxyl moiety and His201α. Their poor activity can be justified by the weakness of all reported interactions. Indeed, the complexes seem stabilized by a precise fitting between the gonanic skeleton and a series of aromatic residues (Tyr361β, Trp106β, Trp303β, and Trp102β) that line the enzymatic cavity rather than by strong and specific interactions with proper amino acidic residues.

Clavaric Acid Derivatives.[31] Lingham et al. have recently isolated from *Clavariadelphus truncatus* a gonanic derivative, the clavaric acid,[32] which is a specific and reversible FTase inhibitor, and they have proposed a series of analogues in order to analyze the structure−activity relationships. We have focused our attention on

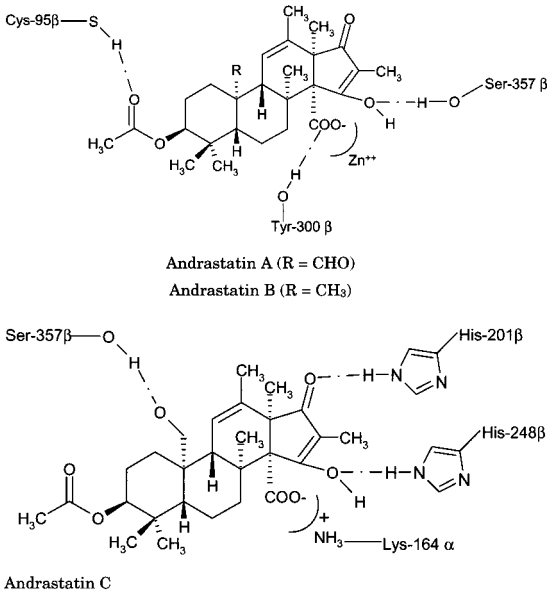

Figure 3. Scheme of main interactions for the andrastatins.

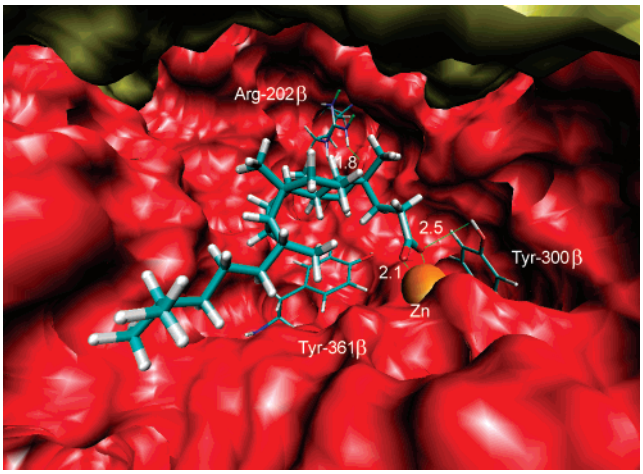

Figure 4. Main interactions between ClavA (1*S*,2*R*) and FTase. The electrostatic interaction between carboxyl moiety and Zn^{2+} ion is notable. The α subunit is shown in yellow and the *β* subunit in red.

Des-A derivatives (i.e., without ring A of gonanic system), since these compounds are principally peptidomimetics, but they become FPP mimetics by adding a succinyl moiety at the 7*β* position. We have examined the two most active molecules: ClavA, peptidomimetic derivative, and ClavB, FPP mimetic. The four possible stereoisomers were considered, as the chirality of C_1 and C_2 is not reported in the literature.

The docking analysis of four isomers of the ClavA derivative shows that those ones with C_2 on R give the better results and so the isomers 1*R*,2*R* and 1*S*,2*R* realize the strongest interactions between ligand oxygenated functions and the residues Tyr-361*β*, His-248*β*, and Arg-202*β*. The C_1 chirality seems to control the ligand ability of directly interacting with Zn^{2+} ion. Indeed, the complex of 1*S*,2*R* (Figure 4) is stabilized by a strong interaction between the Zn^{2+} ion and the carboxyl moiety, while the isomer 1*R*,2*R* does not realize it.

The introduction of the succinyl group in the ClavB derivative improves the obtained complexes, and all ClavB isomers interact with Zn^{2+} ion irrespectively of

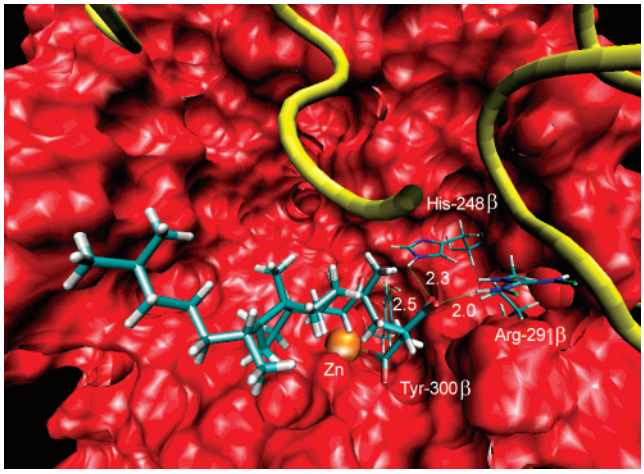

Figure 5. Main interactions between ClavB (1*S*,2*R*) and FTase. Note that the two carboxyl groups perform electrostatic interactions with Zn^{2+} ion and Arg-291*β*. The α subunit is shown in yellow and the *β* subunit in red.

C_1 configuration. Their complexes become stable for several interactions, which involve the functional group of clavaric acid derivatives with Tyr-361*β*, Tyr-300*β*, His-248*β*, Arg-291*β*, and Lys-294*β* (Figure 5).

Discussion: The Site Selectivity

The obtained positions of the natural inhibitors were compared to docking results, earlier determined,[33] for the natural substrates: the farnesylpyrophosphate and the tetrapeptide CVLS, which corresponds to the C-terminal sequence of p21 Ras protein. The substrate positions agree with those experimentally obtained,[34] and it confirms the reliability of the computational method used in this research. The overlapping results, $VO\%_{FPP}$ and $VO\%_{CVLS}$, were expressed as the percentage ratio between common volume and inhibitor volume for both FPP and CVLS, i.e.:

$$VO\%_{FPP} = \frac{V_{inhibitor} \cap V_{FPP}}{V_{inhibitor}} \cdot 100$$

$$VO\%_{CVLS} = \frac{V_{inhibitor} \cap V_{CVLS}}{V_{inhibitor}} \cdot 100$$

The common volumes obtained for considered inhibitors (Table 1) are in good agreement with the experimental observations about their inhibition mechanism, and the results allow to split up the examined natural inhibitor in four main classes.

1. Compounds that have high common volumes for both the natural substrates, like zaragozig acid: these molecules inhibit the FTase occupying both the binding sites without any site specificity. These molecules have high molecular sizes and electron rich groups able to interact with Zn^{2+} ion and specific residues of both binding sites.

2. Compounds that have low common volumes for both the natural substrates, like fusidienol: these molecules inhibit the FTase because they are able to shield selectively the Zn^{2+} ion so that it becomes inaccessible to the natural substrates. Moreover these molecules have a reduced molecular size, but they

Table 1. Overlapping Values of the Considered Compounds with Respect to Positions of CVLS (tetrapeptide corresponding to the C-terminal sequence of p21 Ras protein) and of FPP Expressed as Percentage of Common Volumes, as Well as Lipole Values (hydrophobic momentum) and log *P* Values for Selected Molecules

compound	type[a]	$VO\%_{CVLS}$[b]	$VO\%_{FPP}$[b]	lipole[c]	log *P*[d]
CVLS		100	0	2.2	−0.5
FPP		0	100	*e*	*e*
fusidienol	N.S.	15.7	17.7	1.4	1.8
zaragozic acid	N.S.	41.7	41.3	0.8	2.0
andrastatin a	CVLS	43.3	6.1	2.2	1.7
andrastatin b	CVLS	41	11.9	2.2	1.6
andrastatin c	CVLS	44	6	2.5	2.7
arteminolide	CVLS	47.3	26.9	2.5	1.8
Clav-A 1*S*,2*R*	CVLS	54.7	4.4	2.1	6.0
Clav-B 1*S*,2*R*	FPP	26.5	39.3	4.3	4.2
schizostatin *Z*	FPP	10	36.6	6.7	1.4
schizostatin *E*	FPP	7.1	27.8	6.0	1.3

[a] Inhibition mechanism (from kinetic experiments). N.S. = not selective, CVLS = peptidomimetic, FPP = FPP mimetic. [b] The overlapping values are calculated as a percentage ratio between common volume and molecular volume of inhibitor. [c] The lipole values are calculated according to the hydrophobic momentum formula with the Ghose and Crippen's atomic parameters using VEGA software.[35] [d] The log *P* values are calculated with the MLP method.[36] [e] The log *P* and the lipole for FPP cannot be calculated as the parameters for phosphorus are lacking.

possess functional moieties able to interact with the Zn^{2+} ion and with the cationic residues surrounding it.

3. Compounds that have high common volumes for CVLS tetrapeptide only, like artemidolide: these molecules inhibit the FTase occupying selectively the binding site of peptide substrate, and thus they can be defined as peptidomimetic inhibitors. The ability to compete with this natural substrate seems to be independent of their capacity to achieve a stable interaction with Zn^{2+} ion, but it depends on the possibility to interact (normally by means of H-bonds) with specific residues such as Tyr-361β, Tyr-300β, His-362β, or Ser-357β.

4. Compounds that have high common volumes only for FPP substrate, like schizostatin: these molecules inhibit the FTase occupying selectively the binding site of FPP substrate, and thus they can be defined as FPP mimetic inhibitors. These derivatives compete with the natural substrate realizing electrostatic interactions with the Zn^{2+} ion and with the cationic residues, surrounding it, like Arg-202β, Arg-291β, and Lys-294β.

For all inhibitors, the sum of $VO\%_{FPP}$ and $VO\%_{CVLS}$ is always less than 100 because they can also occupy regions of enzyme cavity different from those occupied by natural substrate. Furthermore, the inhibitors can have a molecular volume less than natural substrates and so they have a sum less than 100 even if they are totally overlapped to natural substrates.

The lipole (*L*) is a measure of the lipophilicity distribution. It can be calculated as sum of local values of log *P*, like dipolar momentum

$$L = \sum_i r_i \cdot l_i$$

where r_i is the distance between atom *i* and the origin of molecule and l_i is the atomic value of the lipophilicity of atom *i*.

This descriptor allows to understand and to predict the different behavior of these natural inhibitors. Indeed, the nonspecific compounds have a low lipole value irrespectively of their molecular size, and the peptidomimetic compounds show a medium lipole, while the FPPmimetic inhibitors possess high values of the lipole. The values shown in Table 1 establish the following:

- molecules with a lipole value less than 2.0 will be not specific inhibitors;
- molecules with a lipole value ranging from 2.0 to 4.0 will probably be peptidomimetics;
- compounds with a lipole value greater than 4.0 will most likely be FPP mimetics.

This observation is very interesting to underline the change from peptidomimetic to FPP mimetic mechanism and justifies the different mechanism for Clav-A and Clav-B compounds. Moreover, the adding of a second carboxylate moiety not only increases the possibility to interact with Zn^{2+} ion but also enlarges the polarity differences between a head hydrophilic and polar and a tail hydrophobic and apolar, likewise the structure of FPP molecule.

Chart 3. Schematic Classification of Natural Ligands in Four Main Classes and Description of Features That Rule This Categorization

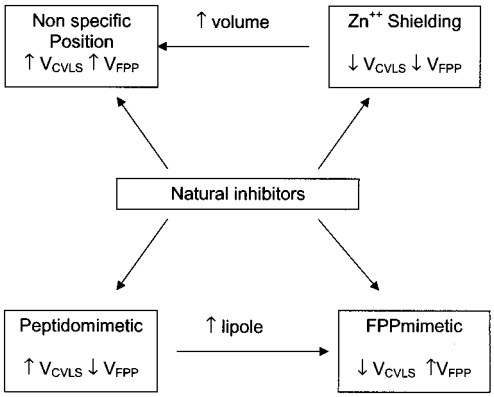

Conclusions

The results of this research show that the molecular docking can be used to explore not only the binding mode of a ligand but also the inhibition mechanism. These results can be achieved comparing the docking orientations for selected inhibitors with the position of natural substrates.

The final results are summarized in Chart 3 where it is possible to see the four main classes of natural inhibitors and the factors that heavily control this subdivision. In this regard, molecular size and lipole seem to be the main factors that rule the change for the nonspecific inhibitors and for peptidomimetics to FPP mimetics. Importantly, the lipole can be used to predict the inhibition mechanism for all examined compounds.

The obtained results also confirm the goodness of computational protocol. In fact, using the combined approach with BioDock and Quanta/CHARMm, it is possible to obtain interesting results in a short time. The BioDock tool provides a lot of possible orientations and performs a preliminary optimization on the best solutions in a limited time, keeping fixed all atoms, whereas the CHARMm minimization analyzes the mutual flexibility for the best complex obtained.

Acknowledgment. The authors acknowledge L. Perri and E. Vocaturo for the computational work during their degree thesis. Thanks are due to A. M. Villa for insightful discussions and L. Fumagalli for carefully reading the English manuscript. This work is supported by Italian MURST.

References

(1) Zhang, F. L.; Casey, P. J. Protein Prenylation: Molecular mechanism and functional consequence. *Annu. Rev. Biochem.* **1996**, *65*, 241−269.
(2) Schafer, W. R.; Kim, R.; Sterne, R.; Thorner, J.; Kim, S. H.; Rine, J. Genetic and pharmacological suppression of oncogenic mutations in Ras genes of yeast and humans. *Science* **1989**, *245*, 379−85.
(3) Zhang, K.; Papageorge, A. G.; Lowy, D. R. Mechanistic aspects of signaling through Ras in NIH 3T3 cells. *Science* **1992**, *257*, 671−674.
(4) Porfiri, E.; Evans, T.; Chardin, P.; Hancock, J. F. Prenylation of Ras proteins is required for efficient hSOS1-promoted guanine nucleotide exchange. *J. Biol. Chem.* **1994**, *269*, 22672−7.
(5) Stimmel, J. B.; Deschenes, R. J.; Volker, C.; Stock, J.; Clarke, S. Evidence for an S-farnesylcysteine methyl ester at the carboxyl terminus of the *Saccharomyces cerevisiae* RAS2 protein. *Biochemistry* **1990**, *29*, 9651−9.
(6) Reiss, Y.; Stradley, S. J.; Gierasch, L. M.; Brown, M. S.; Goldstein, J. L. Sequence requirement for peptide recognition by rat brain p21ras protein farnesyltransferase. *Proc. Natl. Acad. Sci. U.S.A.* **1991**, *88*, 732−736.
(7) Leitner, J. W.; Kline, T.; Carel, K.; Goalstone, M.; Draznin, B. Hyperinsulinemia potentiates activation of p21Ras by growth factors. *Endocrinology* **1997**, *138*, 2211−2214.
(8) Gutierrez, L.; Magee, A. I.; Marshall, C. J.; Hancock, J. F. Posttranslational processing of p21ras is two-step and involves carboxyl-methylation and carboxy-terminal proteolysis. *EMBO J.* **1989**, 1093−8.
(9) Dudler, T.; Gelb, M. H. Palmitoylation of Ha-Ras facilitates membrane binding, activation of downstream effectors, and meiotic maturation in Xenopus oocytes. *J. Biol. Chem.* **1996**, *271*, 11541−7.
(10) Park, H. W.; Boduluri, S. R.; Moomaw. J. F.; Casey. P. J.; Beese. L. S. Crystal Structure of Protein Farnesyltransferase at 2.25 Angstrom Resolution, *Science* **1997**, *275*, 1800−1805.
(11) Chen, W. J.; Andres, D. A.; Goldstein, J. L. Brown, M. S. Cloning and expression of a cDNA encoding the alpha subunit of rat p21ras protein farnesyltransferase. *Proc. Natl. Acad. Sci. U.S.A.* **1991**, *88*, 11368−72.
(12) Chen, W. J.; Andres, D. A.; Goldstein, J. L.; Russell, D. W.; Brown, M. S. cDNA cloning and expression of the peptide-binding beta subunit of rat p21ras farnesyltransferase, the counterpart of yeast DPR1/RAM1. *Cell* **1991**, *66*, 327−34.
(13) Dunten, P.; Kammlott, U.; Crowther, R.; Weber, D.; Palermo, R.; Birktoft, J. Protein farnesyltransferase, structure and implications for substrate binding. *Biochemistry* **1998**, *37*, 7907−12.
(14) Goldstein, J. L.; Brown, M. S.; Stradley, S. J.; Reiss, Y.; Gierasch, L. M. Nonfarnesylated tetrapeptide inhibitors of protein farnesyltransferase. *J. Biol. Chem.* **1991**, *266*, 15575−8.
(15) Gibbs, J. B.; Pompliano, D. L.; Mosser, S. D.; Rands, E.; Lingham, R. B.; Singh, S. B.; Scolnick, E. M.; Kohl, N. E.; Oliff, A. Selective inhibition of farnesyl-protein transferase blocks Ras processing in vivo. *J. Biol. Chem.* **1993**, *268*, 7617−20.
(16) Leonard, D. M. Ras FarnesylTransferase: A New Therapeutic Target. *J. Med. Chem.* **1997**, *40*, 2971−2990.
(17) Halazy, S.; Gotteland, J. P.; Lamothe, M.; Perrin, D.; Hill, B. T. Rationally designed FTase inhibitors. *Drugs Future* **1997**, *20*, 1133−1146.
(18) Omer, C. A.; Kohl, N. E. CaaX competitive inhibitors of farnesyltransferase as anticancer agents. *Trends Pharmacol. Sci.* **1997**, *18*, 437−445.
(19) Qian, Y.; Sebti, S. M. Hamilton, A. D. Farnesyltransferase as a target for anticancer drug design. *Biopolymers* **1997**, *43*, 25−41.
(20) Pedretti, A.; Villa, A. M.; Villa, L.; Vistoli, G. Interactions of some PGHS-2 selective inhibitors with the PGHS-1: an automated docking study by BioDock. *Farmaco* **1997**, *52*, 487−91.
(21) Fantucci, P. C. Personal comunications.
(22) Brooks, B. R.; Bruccoleri, R. E.; Olafson, B. D.; States, D. J.; Swaminathan, S.; Karplus, M. CHARMm: A program for Macromolecular Energy, Minimization and Dynamics Calculations, *J. Comput. Chem.* **1983**, *4*, 187−217.
(23) Stewart, J. P. P. QCPE # 455, free downloadable at http://www.ccl.net.
(24) Quanta/CHARMm, MSI, Burlington, MA.
(25) The software BioDock1.3 is free for academics upon request to the authors.
(26) Sidebottom, P. J.; Highcock, R. M.; Lane, S. J.; Procopiou, P. A.; Watson, N. S. The squalestatins, novel inhibitors of squalene synthase produced by a species of Phoma. II. Structure elucidation. *J. Antibiot.* **1992**, *45*, 648−58.
(27) Singh, S. B.; Jones, E. T.; Goetz, M. A.; Bills, G. F.; Nalli-Omstead, M.; Jenkins, R. G.; Lingham, R. B.; Silverman, K. C.; Gibbs, J. B. Fusidenol: A novel inhibitor of Ras Farnesyl Transferase from fusidium coccineum. *Tetrahedron Lett.* **1994**, *35*, 4963−4969.
(28) Lee, S.; Kim, M.; Bok, S. H.; Lee, H.; Kwon, B.; Shin, J.; Seo, Y. Artemidolide, an inhibitor of Farnesyl Transferase from artemisia sylvatica. *J. Org. Chem.* **1998**, *63*, 7111−7113.
(29) Tanimoto, T.; Onodera, K.; Hosoya, T.; Takamatsu, Y.; Kinoshita, T.; Tago, K.; Kogen, H.; Fujioka, T.; Hamano, K.; Tsujita, Y. Schizostatin, a novel squalene synthase inhibitor produced by the mushroom, *Schizophyllum commune*. I. Taxonomy, fermentation, isolation, physicochemical properties and biological activities. *J. Antibiot.* **1996**, *49*, 617−23.
(30) Uchida, R.; Shiomi, K.; Inokoshi, J.; Sunazuka, T.; Tanaka, H.; Iwai, Y.; Takayanagi, H.; Omura, S. Andrastins, A-C. new protein farnesyltransferase inhibitors produced by Penicillium sp. FO-3929. II. Structure elucidation and biosynthesis. *J. Antibiot.* **1996**, *49*, 418−24.
(31) Lingham, R. B.; Silverman, K. C.; Jayasuriya, H.; Kim, B. M.; Amo, S. E.; Wilson, F. R.; Rew, D. J.; Schaber, M. D.; Bergstrom, J. D.; Koblan, K. S.; Graham, S. L.; Kohl, N. E.; Gibbs, J. B.; Singh, S. B. Clavaric acid and steroidal analogues as Ras- and FPP-directed inhibitors of human farnesyl-protein transferase. *J. Med. Chem.* **1998**, *41*, 4492−501.
(32) Jayasuriya, H.; Silverman, K. C.; Zink, D. L.; Jenkins, R. G.; Sanchez, M.; Pelaez, F.; Vilella, D.; Lingham, R. B.; Singh, S. B. Clavaric acid: a triterpenoid inhibitor of farnesyl-protein transferase from Clavariadelphus truncatus. *J. Nat. Prod.* **1998**, *61*, 1568−70.
(33) Pedretti, A.; Vistoli, G.; Villa, A. M.; Villa, L. Modelling of the interactions of some inhibitors with the farnesyl protein transferase by BioDock − Stochastic approach to automated docking of ligands to biomacromolecules. *Internet J. Chem.* **1999**, *2*, 8.
(34) Strickland, C. L.; Windsor, W. T.; Syto, R.; Wang, L.; Bond, R.; Wu, Z.; Schwartz, J.; Le, H. V.; Beese, L. S.; Weber, P. C. Crystal structure of farnesyl protein transferase complexed with a CaaX peptide and farnesyl diphosphate analogue. *Biochemistry* **1998**, *37*, 16601−11.
(35) VEGA is a homemade software for handling and converting the molecular file formats, and it is free downloadable at http://users.unimi.it/∼ddl.
(36) Gaillard, P.; Carrupt, P. A.; Testa, B.; Boudon, A. Molecular Lipophilicity Potential in 3D-QSAR: Method and Applications. *J. Comput.-Aided Mol. Des.* **1994**, *8*, 83−96.

JM011075W